Individual Object Change Detection for Monitoring the Impact of a Forest Pathogen on a Hardwood Forest

Tim De Chant and Maggi Kelly

Abstract

Sudden oak death (SOD) has caused widespread mortality in a number of tree and shrub species throughout coastal California. As a result, canopy changes are directly visible from remotely sensed imagery. To quantify changes in horizontal canopy structure to the oak woodlands in China Camp State Park, California, USA, a heavily hit area, we developed a novel change detection technique that tracks changes to individual objects. Using 4-band, 1 m spatial resolution aerial photography, we classified four annual images (2000 to 2003) with object-based image analysis (OBIA) and employed a GIS for our change detection technique. We identified 352 gaps that contained SOD mortality in 2000 and persisted through 2003. Their median areas and perimeters did not change significantly in that time. However, those gaps that increased in size tended to be smaller than those that decreased, indicating increased mortality in newly infected areas. Our new change detection method allowed us to monitor these gaps one-by-one, revealing ecologically meaningful results that would otherwise be obscured in a landscape-scale analysis.

Introduction

The forest pathogen *Phytophthora ramorum* has had a significant impact on the forests of central coastal California. Since it was first reported in 1995, it has killed hundreds of thousands of trees, including coast live oak (*Quercus agrifolia*), tanoak (*Lithocarpus densiflorus*), and California black oak (*Q. kelloggii*) (Rizzo *et al.*, 2002; Frankel *et al.*, 2008; Shoemaker *et al.*, 2008). While the pathogen can take anywhere from 2 to 20 years to kill an individual (McPherson *et al.*, 2005), the final decline of the trees has created new openings throughout the affected forests. The pathogen also causes rapid browning of the crown when a canker infection overwhelms the tree, giving it the name "Sudden Oak Death" (SOD) (Rizzo and Garbelotto, 2003). This swift color-change and eventual defoliation of the crown allows the use of remote sensing in the detection of this decline and the tracking of the mortality caused by its progression through the forest (Guo *et al.*, 2007; Kelly, 2003; Kelly and Liu, 2004; Kelly and Meentemeyer, 2002; Kelly *et al.*, 2004; Liu *et al.*, 2007). Treating affected trees and preventing spread of the pathogen on landscape-scales has proved difficult (Davidson *et al.*, 2005). Given this reality, the structure of forests following an infestation has become an important ecological question and one well-addressed by a remote sensing approach. We wanted to investigate the resiliency of the forest canopy in the face of widespread disturbance caused by SOD.

Remote Sensing of Landscape Change

Remote sensing of forest diseases is a relatively new but developed field (Franklin *et al.*, 2000; Pinder and McLeod, 1999). Much of the work has been done on coniferous forests, and there have been a few studies that have looked at pathogens in broad-leaved stands (Everitt *et al.*, 1999; Gong *et al.*, 1999; Guo *et al.*, 2007; Kelly *et al.*, 2004; Liu *et al.*, 2006b). SOD, a relatively new disease, lends itself well to multi-temporal study using remote sensing. Early research focused on monitoring the affected forests (Kelly and McPherson, 2001; Kelly and Meentemeyer, 2002) with later efforts working on increasing the accuracy of correctly identifying dead trees (Guo *et al.*, 2007; Kelly *et al.*, 2004; Liu *et al.*, 2006b; Pu *et al.*, 2008; Sun *et al.*, 2005).

The field of remote sensing has also progressed since work on SOD began, particularly with the broader use of object-based image analysis (OBIA). In the past ten years, three factors have conspired to bring about the development of OBIA (Hay *et al.*, 2005):

1. Computationally intensive OBIA methods are now more accessible given the increase in computing power.
2. High resolution imagery makes object delineation easier for humans and has inspired the development of programs that can assemble pixels into discreet objects.
3. As spatial resolution has increased, individual pixels may no longer be representative of one or more objects but rather a component of a larger feature.

The problems associated with within-object variability is not a new phenomenon (Martin and Howarth, 1989), but the salt-and-pepper effect of pixel-based classifiers is a particular issue when attempting to delineate tree crowns (Kelly *et al.*, 2004). Object-based classification methods have been proven to significantly increase classification accuracy relative to pixel-based methods when mapping overstory mortality in oak woodlands, in part due to their ability to handle within-object variability (Guo *et al.*, 2007). In this

Department of Environmental Science, Policy, and Management, University of California, Berkeley, 137 Mulford Hall, Berkeley, CA 94709 (maggi@berkeley.edu).

Photogrammetric Engineering & Remote Sensing
Vol. 75, No. 8, August 2009, pp. 1005–1013.

0099-1112/09/7508–1005/$3.00/0

study area, with this data, previous research has shown pixel-based methods to be inferior to object-based methods (Kelly *et al.*, 2004; Guo *et al.*, 2007).

OBIA has seen broad application in the field of environmental remote sensing. In a Virginia-based study, it was successful in delineating coniferous, deciduous, and mixed forest stand boundaries using either small-footprint lidar data (0.46 m footprint) or high resolution (1 m) 16-band hyperspectral data (van Aardt and Wynne, 2004). In Siberia, OBIA has also been used to classify areas of deforestation by incorporating proximity to linear features such as roads in the classification (Hese and Schmullius, 2006). In New Mexico, object-based methods have aided in mapping shrub encroachment and its intensity by segmenting the image at varying scales, identifying individual shrubs at finer scales, and then using that data to determine shrub density at coarser scales (Laliberte *et al.*, 2004). Another study used OBIA to map vegetation types (Yu *et al.*, 2006). In the case of this study, OBIA is particularly suited to identifying dead trees in the forest canopy. By segmenting an image into discreet objects, we can not only identify the dead trees, but also outline the extent of their reach.

OBIA methods have also been applied to change detection, but to a lesser extent. One application has been the detection of structural damage due to human conflicts or natural disasters like earthquakes. Object segmentation along with nearest neighbor and fuzzy classification techniques allowed researchers to use 1 and 2 m Ikonos imagery to isolate structures damaged by conflict in Macedonia and the West Bank (Al-Khudhairy *et al.*, 2005). Researchers investigating the aftermath a 1999 earthquake in Turkey found similar success using OBIA in identifying buildings with damage visible from QuickBird imagery (Bitelli *et al.*, 2004). Finally, OBIA has been used with reasonable success in monitoring deforestation in a protected area of the Democratic Republic of Congo. Desclée *et al.* (2004) were able to produce a map of deforestation with 84 percent accuracy by using object-based methods on a multi-date image.

The use of OBIA in change detection, however, is not without challenges. Blaschke (2005) outlines a number of these difficulties:

1. The image's resolution must be sufficiently high to detect the objects of interest, let alone changes that pertain to them.
2. Quality image registration is extremely important. Without this, many perceived changes between two images may simply be due to misregistration.
3. Current accuracy assessment methods are not satisfactorily integrated into the new object-based paradigm. Future research, the paper warns, must take these three issues into account.

While relatively new, object-based change detection techniques are widely varied. Fundamental categories of change detection techniques have been outlined in an extensive review (Lu *et al.*, 2004). Historically, change detection has examined changes on a per pixel basis. OBIA methods can be applied to existing algebraic (image differencing, image regression, etc.) and transformation (principle component analysis, tasseled cap, etc.) approaches, but they can also be applied before any change detection procedures are employed. This paper implements an "Integrated GIS and remote sensing method" by which the segmentation and classification are carried out first, and the change detection is then completed using GIS. It also draws from the spatiotemporal model proposed by Worboys (1992), where the temporal dimension is orthogonal to the 2D representation. This approach is more flexible than a space-time composite (Yuan, 1999) and provides ready access to ancillary data. Our GIS and object-based approach also allowed us to track individual objects as they changed over time, giving us more detailed data that can express more ecological meaning.

Effects of Sudden Oak Death on Forest Structure

Sudden oak death affects two forest types in coastal California, redwood-tanoak forests and coastal California oak woodlands dominated by *Q. agrifolia* and *Umbellularia californica* (Rizzo and Garbelotto, 2003). SOD has affected *Q. agrifolia* with larger stem diameters more than smaller ones, a characteristic of the disease that has pushed the size distribution of affected populations down. Previous work on gap dynamics in California oak woodlands suggests that oaks may need a shrub-dominated stage for successful recruitment (Callaway and Davis, 1998), but few studies to date have examined such events following SOD (but, see Brown and Allen-Diaz, 2008).

Most research into gap dynamics in oak woodlands has examined recruitment (Asbjornsen *et al.*, 2004b; Callaway and Davis, 1998) and microclimatic effects (Asbjornsen *et al.*, 2004a) with few focusing on changes in canopy structure (Clinton *et al.*, 1993). With SOD removing larger trees from the canopy in a spatially contagious pattern (Kelly and Meentemeyer, 2002; Kelly *et al.*, 2008), the openings are concentrated in some areas while relatively sparse in others, creating a gradient of disturbance.

We used a new object-by-object (OBO) change detection technique to quantify changes in horizontal canopy structure of individual gaps following mortality caused by *P. ramorum*. We expected the OBO technique to reveal more detailed information about the canopy gap structure through time than a landscape-only approach. Specifically, we used OBIA to delineate, classify, and structurally quantify individual changes in canopy gaps between 2000 and 2003 that were caused by *P. ramorum* mortality in 2000. As mortality continued between 2000 and 2003, we anticipated that gap size would continue to increase. We considered lateral recruitment a factor that would potentially balance out some of the increases in gap size due to ongoing mortality. Finally, we predicted that larger gaps will continue to grow as a result of mortality and increasingly stressful microclimatic conditions, while the smaller gaps will decrease in size.

Methods

Study Site

The study area for this project is 1,340 ha of a forested peninsula in eastern Marin County (Figure 1). Jutting eastward into San Pablo Bay, the woodlands on the peninsula are managed in the northwest by Marin County Open Space as San Pedro Ridge Reserve, in the southwest by the City of San Rafael as Henry A. Barbier Park, and in the east by the California State Parks as China Camp State Park. While under separate jurisdictions and different official names, these three areas are commonly referred to as China Camp. A large portion of the open space on the peninsula features near even-aged stands containing *Q. agrifolia*, *Q. kelloggii*, and *Q. lobata* along with *Arbutus menziesii* and *Umbellularia californica*. Of these, *Q. lobata* is the only non-host species for *P. ramorum*. These stands are spread across a landscape with moderate to steep topography rising from sea level to over 300 m in elevation.

Imagery Acquisition and Registration

We acquired digital imagery for China Camp annually from 2000 to 2003 through private contractors (Positive Systems, Inc. and ARINC, Inc.). The imaging system was an ADAR 5500 that has an SN4, 20 mm lens with four mounted cameras with

Figure 1. The China Camp study area located in Marin County on the western shore of San Pablo Bay.

four corresponding spectral bands (Blue: 450 to 550 nm, Green: 520 to 610 nm, Red: 610 to 900 nm, and Near Infrared (NIR): 780 to 920 nm). The aircraft was flown at an average altitude of 2,205 ft. AGL, giving each 1,000 m × 1,500 m frame an average ground spatial resolution of 1 m. Each frame has 35 percent side- and 35 percent end-lap. The imagery used in this study was acquired between the months of March and May for each year both to reduce the confusion between dead trees and California buckeye, a summer deciduous tree, and to capture the springtime canopy cover change caused by SOD.

The frames for each year were mosaicked and georeferenced using a 6-inch resolution digital orthophotograph of the county provided by the Marin Municipal Water District. Positive Systems registered each year to an accuracy of 0.305 m. Further registration was performed to minimize interannual variations according to Liu *et al.* (2006a). This automated registration technique uses local area-based control point extraction and a local transformation model (the piecewise linear model). All images were registered to the 2001 image. Interannual RMSE was calculated in ERDAS Imagine® software (ERDAS, 1999) using 10 control points. RMSE between 2000 and 2001 was 1.83 m, 2.16 m for 2001 to 2002, and 3.02 m for 2001 to 2003.

Imagery Enhancement and Segmentation

A number of indices and enhancements were applied to the mosaicked and registered images using ERDAS Imagine® software (ERDAS, 1999) and evaluated. Of these, two were useful: Normalized Difference Vegetation Index (NDVI) and intensity, hue, and saturation (IHS). NDVI was originally developed for Thematic Mapper data from the Landsat satellites (Crist, 1985), but ADAR's similarity in spectral resolution allowed us to employ it. The second enhancement, IHS, recoded the original NIR-red-green-blue image into intensity-hue-saturation. All of these layers, including the original four-band imagery, were then loaded into Definiens Professional 5.0 (Definiens, 2006), an object-based image analysis software package also known as eCognition®. See Table 4 for a detailed list of which bands, enhancements, and other features that were used in the classification.

The image was segmented at two scales (scale = 15 and scale = 8) using all four spectral bands. NIR was given the highest weight in segmentation (1.0) due to the spectral differences between live and dead crowns. The remaining layers (RGB) were all weighted lower (0.3). The second level (scale = 8) was fine enough to isolate individual dead trees from the surrounding canopy (Figure 2).

Classification of the Imagery

The larger scale (scale = 15, Level 15) was used to mask non-vegetation objects from areas of vegetation. Non-vegetation objects most often consisted of urban land cover (houses, roads, etc.) but also included areas of bare soil and hiking trails. At the smaller scale (scale = 8, Level 8, Figure 3), the objects from Level 15 were broken into more detailed classes. The classes for the 2000 image included Trees, Dead Trees, Dead Trees (Neighbor), Not Vegetation, Other Vegetation, and Shadows; although Shadows and Other Vegetation were merged for the purposes of gap analysis. Data from Liu *et al.* (2006b) was brought in as a thematic layer to enhance classification by reducing misclassification of deciduous trees as dead trees (Dead Trees). Dead Trees also used the *Ratio* feature in eCognition®, where the ratio of the spectral feature of interest is compared to all other spectral bands and enhancements from the image. Dead Trees (Neighbor) used the same shape and spectral rules as Dead Trees, but also used a "Neighbor to *Dead Trees*" rule to capture mortality that had not been included in the thematic layer from Liu *et al.* (2006b). For a detailed look at the use of topological relationships in OBIA, see Liu *et al.* (2008). The Dead Trees and Dead Trees (Neighbor) classes consisted of standing dead trees; trees with catastrophic failures or snapped stems were classified as Other Vegetation. In this study, overstory

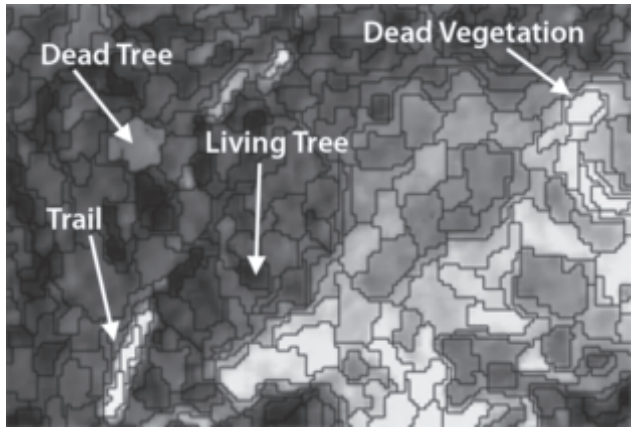

Figure 2. Image segments created by eCognition® at scale = 8. Note the slightly lighter color of the dead tree in the middle of the image and its contrast with the bright white of the trail in the lower left.

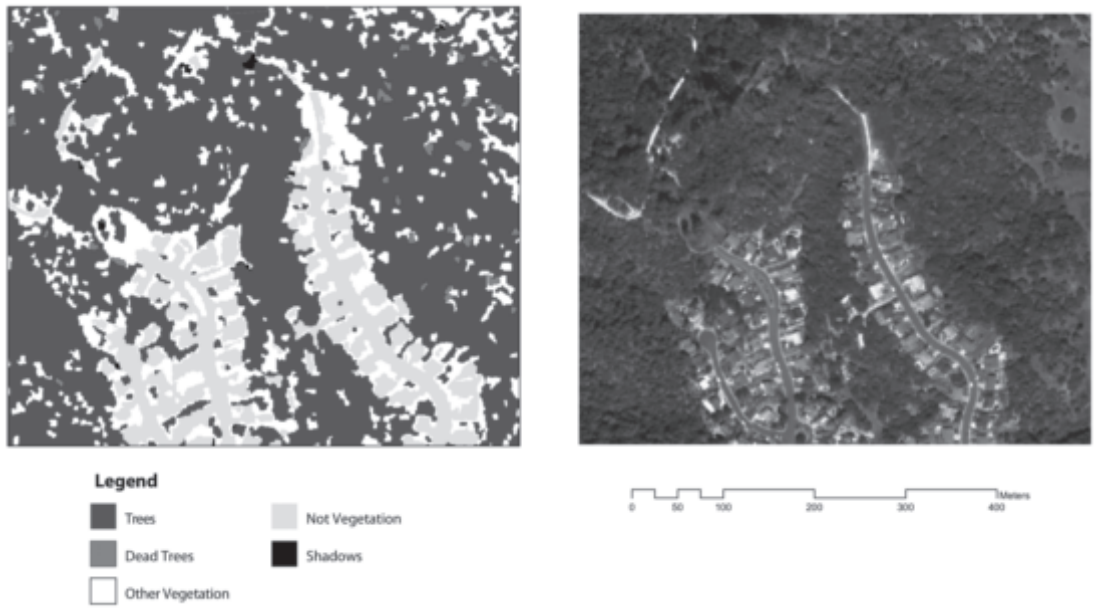

Figure 3. Sample of the classified image from 2000 at scale = 8 (a), and the red band from the original image (b). For this image, Dead Trees and Dead Trees (Neighbor) were merged for clarity, resulting in five total classes.

mortality is assumed to be caused by *P. ramorum* based on the findings of Swiecki and Bernhardt (2002).

The Dead Trees and Dead Trees (Neighbor) classes were extracted in a GIS and intersected with polygons from a two-class reclassification scheme: (a) Trees, which contained the original Trees class, and (b) Not Trees, which contained the original classes Other Vegetation, Not Vegetation, Shadows, and Dead Trees. This was done to determine which gaps contained trees killed by *P. ramorum* so as to track them in the subsequent imagery (2001 to 2003). To assess classification accuracy, we generated 50 random points per class using the Hawth's Tools (Beyer, 2004) for ArcMap® (ESRI, Inc., Redlands, California) across all five classes (Trees, Other Vegetation, Not Vegetation, Dead Trees, Dead Trees (Neighbor), and Shadows) for the year 2000 and two classes for 2001 to 2003 (assessing the two-class reclassification: Trees and Not Trees). The status of those points was visually assessed from the digital imagery. A two-meter buffer was included around these points to account for up to two pixels of variation in the segmentation process.

Spatial Analysis and Processing of Gap Data

Polygons classified as gaps (Not Vegetation, Other Vegetation, Dead Trees, Dead Trees (Neighbor)) were merged into continuous objects and exported from eCognition® as raster data. Once exported, Fragstats (McGarigal *et al.*, 2002) was used to determine each individual gap's area, perimeter and Euclidean nearest neighbor (ENN). The raster output from Fragstats for each year was then converted to a shapefile and imported into a PostGIS database (Refractions Research, 2005), an open-source spatially-aware relational database. In PostGIS, we intersected gap polygons from 2000 with polygons classified as Dead Trees and Dead Trees (Neighbor). We isolated the gap polygons from the 2000 image that contained dead trees and intersected them with gap polygons from 2001, 2002, and 2003 using a Perl script and the "intersects" function in PostGIS. Those that spatially intersected were uniquely identified. The output of this script was then used to pair each individual gap to its Fragstats data. See Figure 4 for a visual representation of these methods.

Many gaps did not split or merge over the four years (Figure 5; Example B). But there were gaps that did split or

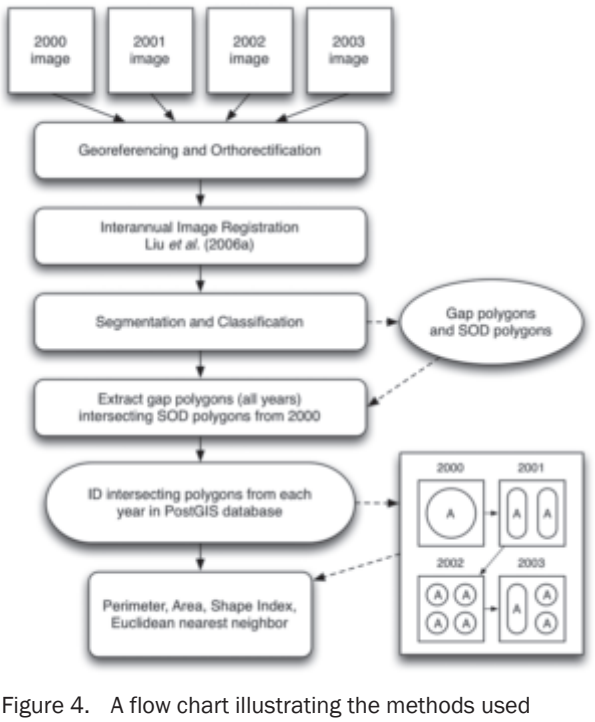

Figure 4. A flow chart illustrating the methods used in this study.

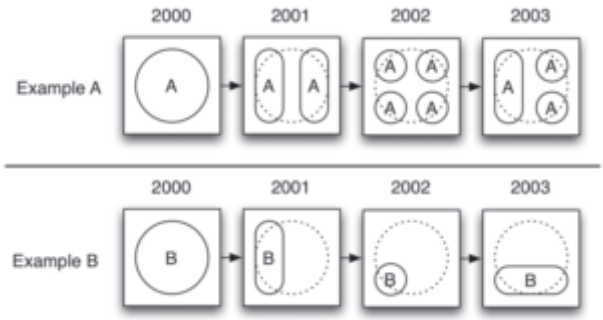

Figure 5. Two hypothetical gap polygons and their respective fates from 2000 to 2003. *Example A* (top) is begins as one gap in 2000. Its original boundary is represented as a dashed circle in following years for reference. In 2001, the gap splits into two. In 2002, those two gaps then each split into two more gaps. In 2003, the left two gaps merge, leaving three remaining gaps. Although each gap is distinct in its own year, it is related to its neighbors through its overlap with the original gap in 2000. Thus, all gaps overlapping with *A* in 2000 are identified as *A* in subsequent years. *Example B* (bottom) illustrates the other fate of a gap originating in 2000 (shown as a dashed circle in following years for reference). It begins and remains as one gap throughout the study, but changes in size and shape.

merge (Figure 5; Example A). The landscape metrics of those that split or merged needed additional processing. These gaps had been uniquely identified using the Perl/PostGIS processing detailed above, creating an association of gaps within a year that shared an intersection with a polygon or polygons from another year. Data from these associations were aggregated: areas and perimeters were summed, ENN distances were averaged, and shape index (SI) was calculated from the summed areas and perimeters. These landscape metrics were then analyzed over three different time scales: annually, biannually (2000 to 2002 and 2001 to 2003), and over the entire study (2000 to 2003).

Gaps over 3 ha were discarded from further analysis as they were primarily caused by urbanization. Three hectares is above what has been previously considered in the literature (e.g., Hubbell *et al.*, 1999; Yamamoto, 1993), but this threshold was kept due to the fractal nature of many of the larger (>0.2 ha) SOD containing gaps.

Statistical Tests

The resulting data for all measures of gap structure were significantly non-normal by the Wilks-Shapiro W test in JMP 5.1.2 (SAS Institute, Inc., 2005). As a result, parametric methods were discarded in favor of the Wilcoxon rank sum test and Hodges-Lehman estimators in R (R Development Core Team, 2008), both of which are robust in the face of non-normality. As such, all results for these tests listed below that indicate significant changes in particular metrics are median changes.

We also investigated how changes in landscape metrics over the study period were influenced by gap characteristics in 2000. For example, we were interested in how gap metrics in 2000 may influence changes in gap area over the course of the study period. Wilcoxon rank sum tests show significant differences in all metrics between gaps that increased in size compared to those that decreased in size over the study period. To identify which metrics in 2000 had the most influence on the change in metrics over time, we used recursive partitioning and tree pruning to determine the most significant effects (R Development Core Team, 2008). Two models were constructed, one with area, perimeter, and ENN and the other with SI and ENN (SI is derived from area and perimeter, so the three could not be combined in the same model).

Results

Overall accuracies for the classified images were 95 percent for 2000, 97 percent for 2001, and 98 percent for 2002 and 2003 (Tables 1 and 2). Most classes had high accuracy in classification. Dead Trees (Neighbor) in the 2000 image is a minor exception, with that class most often confused for Other Vegetation or Shadows. Overall Kappa statistics for the images were 0.94 for 2000, 0.9417 for 2001, and 0.9608 for 2002 and 2003.

The classified and post-processed imagery returned a total of 352 gaps and associations that contained SOD mortality in 2000 and persisted until 2003. In 2000, those gaps occupied 10.736 ha and made up 44.13 km of forest edge. In 2003, those numbers dropped to 6.122 ha and 34.682 km, respectively. This landscape level data, however, only describes part of the story. The individual gap areas, perimeters, shape indices, and ENN measurements show range of significant changes that varies depending on the time scale over which they were tested.

Annual Time Scale

We first analyzed the gaps' and associations' landscape metrics on an annual time scale (e.g., 2000 to 2001). Between 2000 and 2001, area of the individual gaps and associations

TABLE 1. CONFUSION MATRIX FOR CLASSIFICATION OF 2000: T = TREES, OV = OTHER VEGETATION, DT = DEAD TREES, DTN = DEAD TREES (NEIGHBOR), NV = NOT VEGETATION, S = SHADOWS

	T	OV	DT	DTN	NV	S	Total	Omission (%)
T	49	0	0	0	0	1	50	98
OV	0	46	1	0	2	1	50	92
DT	1	1	48	0	0	0	50	96
DTN	0	4	0	43	0	3	50	86
NV	0	1	0	0	49	0	50	98
S	0	0	0	0	0	50	50	100
Total	50	52	49	43	51	55	285	
Commission (%)	98	88.46	97.96	100	96.08	90.91		

Overall Accuracy = 95% (285/300), Khat = 0.94

TABLE 2. CONFUSION MATRIX FOR CLASSIFICATIONS OF 2001 TO 2003 WITH OVERALL ACCURACY AND KAPPA COEFFICIENTS

Class		Trees	Not Trees	Total	Omission
Trees	2001	50	0	50	100%
	2002	50	0	50	100%
	2003	49	1	50	98%
Not Trees	2001	3	47	50	94%
	2002	2	48	50	96%
	2003	1	49	50	98%
Total	2001	53	47	97	
	2002	52	48	98	
	2003	50	50	98	
Commission	2001	94.34%	100%		
	2002	96.15%	100%		
	2003	98%	98%		
		2001	2002	2003	
	Overall	97%	98%	98%	
	Khat	0.9417	0.9608	0.9608	

significantly increased by 11 m^2; perimeter, SI, and ENN did not show any significant changes. The next year (2001 to 2002), no significant changes occurred in any metric. For the final year (2002 to 2003), both area and perimeter decreased significantly (12 m^2 and 8 m, respectively) while SI significantly decreased by 0.113. ENN for the final year increased by 0.83 m (Table 3).

Variable Time Scale

When analyzing different blocks of time, we noticed a different set of changes in the landscape metrics. For the first two year time span (2000 to 2002), three metrics showed significant increases: area (14 m^2), perimeter (6 m), and ENN (0.63 m). When the same time span was shifted to the latter dates of the study (2001 to 2003), only ENN distances increased (0.94 m) while the rest decreased (area by 9 m^2, perimeter by 6 m, and SI by 0.09). These different two year windows disparate results are likely heavily influenced by their composite years, with 2000 to 2001 and 2002 to 2003 contributing the bulk of the changes as no metrics between 2001 to 2002 showed any differences (Table 3).

We then integrated the results over the entire time span of the study (2000 to 2003), and another trend emerged. Perimeter and area drop out of significance while ENN distances increased by 0.93 m and SI decreased by 0.097 (Table 3).

Influence of Metrics in 2000 on Metrics in 2003

We tested two recursive partitioning models with tree pruning to determine how gap area in 2000 influenced gap area in 2003. One model (SI and ENN) kept both SI and ENN as significant predictors of change in area between 2000 and 2003, but the splits hold little sensible explanatory power. The other model (Area, Perimeter, and ENN) kept area as the most significant predictor of change in area, dropping perimeter and ENN. In this model, canopy gaps greater than or equal to 147.5 m^2 decreased in size while those smaller than this number increased. This confirms the results of the Wilcoxon tests for increasing and decreasing gaps, but shows that only area is significant when the other metrics are included in the model.

Discussion

This new change detection technique allowed us to track 352 canopy gaps and gap associations individually and provided us with more detailed information about the woodland's

TABLE 3. MEDIAN DIFFERENCES IN GAP METRICS YEAR TO YEAR (a), AND OVER VARYING TIME FRAMES (b)

	Area (m^2)	Perimeter (m)	Shape Index	ENN (m)
2000–2001	11.00**	—	—	—
2001–2002	—	—	—	—
2002–2003	−12.00**	−8.00**	−0.11**	0.83***

—: no significant differences* $p < 0.05$ ** $p < 0.01$ *** $p < 0.001$

(a)

		Area (m^2)	Perimeter (m)	Shape Index	ENN (m)
1 year	2000–2001	11.00**	—	—	—
2 years	2000–2002	14.00***	6.00*	—	—
	2001–2003	−9.00*	−6.00*	−0.09**	0.94***
3 years	2000–2003	—	—	−0.097**	0.93***

—: no significant differences* $p < 0.05$ ** $p < 0.01$ *** $p < 0.001$

(b)

changing spatial structure than a landscape-only method. Tracking changes to objects of varied sizes would not be possible using traditional pixel-based classification methods, nor would it be possible using landscape-scale quantification. Our results chart the changes of gaps at a variety of scales. While other fields have explored tracking objects through time (Croitoru *et al.*, 2006), it is relatively new to ecology. Our study adds a new approach to studying numerous small-scale changes on the landscape in great detail.

The large number of gaps that contained one or more dead trees in 2000 is indicative of the impact SOD has had on the over 900 ha of forested land in the China Camp area. The spatially contagious nature of the disease should logically lend itself to increasing gap size over the course of the study, but our results indicate the resiliency of the overall canopy structure at China Camp. This pathogen has increased the dynamism of the horizontal canopy structure, but the forest has rebounded relatively quickly to fill in the gaps shortly after they open.

Previous research into the impact of SOD on forest structure has been limited to a landscape-only assessment (Kelly and Meentemeyer, 2002; Liu *et al.*, 2007), revealing the pathogen's spatially contagious nature. But these studies did not reveal details on how the disease is affecting the horizontal canopy structure of the forest. Furthermore, this study is the first to study the changes of individual gaps over a multi-year time span. The use of OBIA techniques gave us high classification accuracies for all of our images. Our results agree with a previous study at the same site using the same imagery (Guo *et al.*, 2007) and also are in line with other OBIA classification schemes using similar imagery (Desclée *et al.*, 2004).

OBIA provided us with ecologically meaningful objects, including polygons that outlined the crowns of still-standing dead trees that were absent any salt-and-pepper effects from bare soil showing through the bare branches. Additionally, we chose OBIA for its ability to segment and classify at different scales. Many of the dead trees were spectrally similar to some of the rooftops of houses in the adjacent residential areas. By first segmenting and classifying at a larger scale (scale = 15), we were able to mask the residential areas in the Not Vegetation class using hierarchical classification rules. We selected our lower scale parameter (scale = 8), based on the quality of segmentation for tree crowns. These two scales complimented each other through the hierarchical rules: The higher parameter undersegmented dead tree crowns (lumping them in with other vegetation) while properly segmenting residential areas. The lower scale parameter then properly segmented the dead tree crowns suspected to be caused by SOD.

We expected gaps containing SOD to increase in size over the course of the study, but the lack of significant difference between 2000 and 2003 in median individual gap area disproves this hypothesis. The total gap area affected by SOD in 2000 decreased by a large amount over the study period (almost 4 ha), but the median gap size for the individual gaps did not change. In fact, only shape index and Euclidean nearest neighbor differed between 2000 and 2003. The change in SI indicates that the gaps are becoming more regular in shape. This change could be due to trees with more edge exposure dying off, but it is more likely that the more irregular gaps' lobes are being closed by the surrounding trees. The median increase in ENN is another sign that the forest is responding rapidly, filling small gaps that may have been present in 2000 but did not persist through the study period to 2003.

The differing results from the varying time frames (1, 2, and 3 years) and the varying applications of those time frames (e.g., 2000 to 2002 and 2001 to 2003) highlight two interesting points. First, the length of the time frame is important in understanding the dynamics of the system. This is nothing new to ecology (Delcourt *et al.*, 1983), but our findings further reinforce how important these decisions are, even on the micro-scale. We were limited to four images over three years due to data availability; had we been limited to three images over two years (2000 to 2002), we may have drawn drastically different conclusions. Over that two year period, median gap area increased 14 m^2 compared to no significant changes in median area over the 2000 to 2003 time frame. This high degree of variability in results over relatively short times spans also points to the dynamic nature of China Camp's oak woodlands.

Second, the division of the data into separate analytical frames can help to highlight which time frames exert more or less influence on the outcome of the entire study period. Between 2000 and 2001, for example, median gap area increased 11 m^2. In 2001 to 2002, no significant change in area was seen. For the last year (2002 to 2003), area decreased by a median of 12 m^2, effectively canceling out the growth in the first year (change area was insignificant over the entire study period). This indicates that China Camp's oak woodlands exhibited heavy lateral recruitment that likely offset continuing SOD mortality.

Over the three years of this study, smaller gaps were expected to decrease in size while larger gaps were expected to increase. This was predicted due to the hot, dry summers China Camp experiences, increasing drought stress in the larger, less sheltered gaps. Interestingly, the exact opposite occurred. Smaller gaps ($<$147.5 m^2) continued to increase in size between 2000 and 2003 while larger gaps ($\geqslant$147.5 m^2) decreased in size. This result could have arisen from one of three possible conditions or a combination thereof:

1. Microclimatic conditions in China Camp are not as extreme as originally anticipated, or the trees growing there are well adapted to Mediterranean summers.
2. SOD, with its spatially contagious distribution (Kelly and Meentemeyer, 2002) and limited dispersal ability (except for sporadic long range dispersal events; Mascheretti *et al.*, 2008) continues to spread to vulnerable hosts bordering the smaller gaps while it has largely exhausted the vulnerable hosts on the edges of the large gaps.
3. Microclimatic conditions or species assemblages in the larger gaps are hotter and drier, conditions that are less suitable for transmission of *P. ramorum* (Swiecki and Bernhardt, 2002).

It is likely that these three explanations compliment each other, with each one contributing to the trend of smaller gaps growing while larger gaps shrink.

Conclusions

This study bridges both ecology and remote sensing. On the ecological front, we investigated the effects of a widespread forest pathogen in the oak woodlands of California, Sudden Oak Death. We used high-resolution imagery both to test our ecological hypotheses about canopy gap structure through time and to test our new approach to change detection, i.e., object-by-object (OBO) change detection. OBO change detection identifies individual polygons in the first image of the series and tracks their change through the subsequent images, producing results that detail the changes of these gaps individually and not in aggregate. This study is the first of its kind to track changes in forest canopy gap structure on an individual basis. The successful characterization of the individual canopy gaps throughout the study has lent insight into the dynamics of California's coastal oak woodlands in the wake of SOD. The oak woodlands at China Camp have rebounded considerably, both reducing the total size of all gaps that contained SOD. At smaller scales, the median gap

TABLE 4. CLASSES (LEFT) WITH THE BANDS (NIR, RED, GREEN, BLUE), ENHANCEMENTS (HUE, RATIO HUE, RATIO BLUE), THEMATIC LAYERS (SUSPECTED DEAD TREES - BASED ON DATA FROM LIU *ET AL.*, 2006B), SPATIAL (ROUNDNESS, AREA, NEIGHBOR TO *DEAD TREES*), HIERARCHICAL (EXISTENCE OF *NOT VEGETATION* AT LEVEL 15) AND OTHER SPECTRAL INFORMATION (BRIGHTNESS)

Class	Features used
Trees	NDVI
Other Vegetation	NIR, NDVI, Not *Trees*
Dead Trees	NIR, NDVI, Roundness, Area, Ratio Hue, Suspected Dead Trees (thematic layer)
Dead Trees (Neighbor)	NIR, NDVI, Roundness, Area, Ratio Hue, Neighbor to Dead Trees
Not Vegetation (Level 8)	Existence of *Not Vegetation* at Level 15
Shadows	Brightness, Ratio Hue
Vegetation (Level 15)	Not *Not Vegetation* at Level 15
Not Vegetation (Level 15)	NDVI, Ratio NIR, Ratio Blue

size has remained constant even as the pathogen continues to kill mature trees, an ecologically significant finding that is a direct product of the OBO change detection technique. While SOD will certainly affect the species composition of California's coastal oak woodlands, the remaining forest structure shows remarkable resiliency in the face of this disturbance.

Acknowledgments

We would like to thank several people who helped with the preparation of this manuscript: Desheng Liu for use of his automated registration technique and SOD data (see Table 4), Marek Jakubowski for his help in scripting the unique identification of related gaps, and Brent Pedersen for his help troubleshooting the Perl script. The paper was greatly strengthened by the suggestions of two anonymous reviewers. Finally, we are grateful for research support from the U.S. Department of Agriculture.

References

Al-Khudhairy, D.H.A., I. Caravaggi, and S. Giada, 2005. Structural damage assessments from IKONOS data using change detection, object-oriented segmentation, and classification techniques, *Photogrammetric Engineering & Remote Sensing*, 71(7):825–837.

Asbjornsen, H., M.S. Ashton, D.J. Vogt, and S. Palacios, 2004a. Effects of habitat fragmentation on the buffering capacity of edge environments in a seasonally dry tropical oak forest ecosystem in Oaxaca, Mexico, *Agriculture, Ecosystems and Environment*, 103:481–495.

Asbjornsen, H., K.A. Vogt, and M.S. Ashton, 2004b. Synergistic responses of oak, pine and shrub seedlings to edge environments and drought in a fragmented tropical highland oak forest, Oaxaca, Mexico, *Forest Ecology and Management*, 192:313–334.

Beyer, H.L. 2004. Hawth's Analysis Tools for ArcGIS, URL: *http://www.spatialecology.com/htools* (last date accessed: 04 May 2009).

Bitelli, G., R. Camassi, L. Gusella, and A. Mognol, 2004. Image change detection on urban area: The earthquake case, *Proceedings of the International Society for Photogrammetry and Remote Sensing*, 12–23 July, Istanbul, Turkey.

Blaschke, T., 2005. Towards a framework for change detection based on image objects, *Remote Sensing & GIS for Environmental Studies* (S. Erasmi, B. Cyffka, and M. Kappas, editors), Göttinger Geographische Abhandlungen, Göttingen, Germany.

Brown, L., and B. Allen-Diaz, 2008. Forest response to an emerging disease: Sudden oak death in coastal California, *Proceedings of the Sixth California Oak Symposium*, 09–12 October 2006, Rohnert Park, California (U.S. Department of Agriculture, Albany, California).

Callaway, R.M., and F.W. Davis, 1998. Recruitment of *Quercus agrifolia* in central California: The importance of shrub-dominated patches, *Journal of Vegetation Science*, 9:647–656.

Clinton, B.D., L.R. Boring, and W.T. Swank, 1993. Canopy gap characteristics and drought influences in oak forests of the Coweeta Basin, *Ecology*, 74(5):1551–1558.

Croitoru, A., K. Eickhorst, A. Stefandis, and P. Agouris, 2006. Spatiotemporal event detection and analysis over multiple granularities, *Progress in Spatial Data Handling: 12th International Symposium on Spatial Data Handling*, 12–14 July, Vienna, Austria.

Crist, E.P., 1985. TM tasseled cap equivalent information for reflectance factor data, *Remote Sensing of Environment*, 17(3):301–306.

Davidson, J.M., A.C. Wickland, H.A. Patterson, K.R. Falk, and D.M. Rizzo, 2005. Transmission of *Phytophthora ramorum* in mixed-evergreen forest in California, *Ecology and Epidemiology*, 95(5):587–596.

Definiens, 2006. *Definiens Professional 5 Reference Book*, Definiens AG, Munich, Germany, 122 p.

Delcourt, H.R., P.A. Delcourt, and T. Webb, III, 1983. Dynamic plant ecology: The spectrum of vegetational change in space and time, *Quaternary Science Reviews*, 1(3):153–175.

Desclée, B., P. Bogaert, and P. Defourny, 2004. Object-based methods for automatic forest change detection, *Proceedings of Geoscience and Remote Sensing Symposium (IGARSS '*04), 20–24 September, Anchorage, Alaska (IEEE International, New York), 3383–3386.

ERDAS, 1999. *ERDAS Field Guide*, ERDAS, Inc., Atlanta, Georgia, 672 p.

Everitt, J., D. Escobar, D. Apple, W. Riggs, and M. Davis, 1999. Using airborne digital imagery for detecting oak wilt disease, *Plant Disease*, 83:502–505.

Frankel, S.J., 2008. Sudden oak death and *Phytophthora ramorum* in the USA: A management challenge, *Australasian Plant Pathology*, 37(1):19–25.

Franklin, J., C.E. Woodcock, and R. Warbington, 2000. Multi-attribute vegetation maps of forest service lands in California supporting resource management decisions, *Photogrammetric Engineering & Remote Sensing*, 66(10):1209–1217.

Gong, P., X. Mei, G.S. Biging, and Z. Zhang, 1999. Monitoring oak woodland change using digital photogrammetry, *Journal of Remote Sensing*, 3:285–289.

Guo, Q., M. Kelly, P. Gong, and D. Liu, 2007. An object-based classification approach in mapping tree mortality using high spatial resolution imagery, *GIScience & Remote Sensing*, 44(1):24–47.

Hay, G.J., G. Castilla, M.A. Wulder, and J.R. Ruiz, 2005. An automated object-based approach for the multiscale image segmentation of forest scenes, *International Journal of Applied Earth Observation and Geoinformation*, 7:339–359.

Hese, S., and C. Schmullius, 2006. Object context information for advanced forest change classification strategies, *1st International Conference on Object-based Image Analysis*, 04–05 July, Salzburg, Austria

Hubbell, S.P., R.B. Foster, S.T. O'Brien, K.E. Harms, R. Condit, B. Wechsler, S.J. Wright, and S. Loo de Lao, 1999. Light-gap

disturbances, recruitment limitation, and tree diversity in a neotropical forest, *Science*, 283:554–557.

Kelly, M., 2003. Terrain modeling and visualization to understand spatial pattern and spread of sudden oak death in California, *Proceedings of the ASPRS Terrain Data Conference*, 24–29 October, Charleston, South Carolina (American Society for Photogrammetry & Remote Sensing, Bethesda, Maryland), pp. 13–24.

Kelly, M., and D. Liu, 2004. Mapping diseased oak trees using ADAR imagery, *Geocarto International*, 19(1):57–64.

Kelly, M., D. Liu, B. McPherson, D. Wood, and R. Staniford, 2008. Spatial pattern dynamics of oak mortality and associated disease symptoms in a California hardwood forest affected by sudden oak death. *Journal of Forest Research* 13(5):312–319

Kelly, M., and B.A. McPherson, 2001. Multi-scale approach taken to sudden oak death monitoring, *California Agriculture*, January-February:15–16.

Kelly, M., and R. Meentemeyer, 2002. Landscape dynamics of the spread of sudden oak death, *Photogrammetric Engineering & Remote Sensing*, 68(10):1001–1009.

Kelly, M., D. Shaari, Q. Guo, and D. Liu, 2004. A comparison of standard and hybrid classifier methods for mapping hardwood mortality in areas affected by sudden oak death, *Photogrammetric Engineering & Remote Sensing*, 70(11):1229–1239.

Laliberte, A.S., A. Rango, K.M. Havstad, J.F. Paris, R.F. Beck, R. McNeely, and A.L. Gonzalez, 2004. Object-oriented image analysis for mapping shrub encroachment from 1937 to 2003 in southern New Mexico, *Remote Sensing of Environment*, 93(1–2):198–210.

Liu, D., P. Gong, M. Kelly, and Q. Guo, 2006a. Automatic registration of airborne images with complex local distortion, *Photogrammetric Engineering & Remote Sensing*, 72(9):1049–1060.

Liu, D., M. Kelly, and P. Gong, 2006b. A spatial-temporal approach for monitoring forest disease dynamics using multi-temporal high spatial resolution imagery, *Remote Sensing of Environment*, 101(2):167–180.

Liu, D., M. Kelly, P. Gong, and Q. Guo, 2007. Characterizing spatial-temporal tree mortality patterns associated with a new forest disease, *Forest Ecology and Management*, 253(1–3):220–231.

Liu, Y., Q. Guo, and M. Kelly, 2008. A framework of region-based spatial relations for non-overlapping features and its application in object based image analysis, *ISPRS Journal of Photogrammetry & Remote Sensing*, 63(4):461–475.

Lu, D., P. Mausel, E. Brondízio, and E. Moran, 2004. Change detection techniques, *International Journal of Remote Sensing*, 20(12):2365–2407.

Martin, L.R.G., and P.J. Howarth, 1989. Change-detection accuracy assessment using SPOT multispectral imagery of the rural-urban fringe, *Remote Sensing of Environment*, 30(1):55–66.

Mascheretti, S., P.J.P. Croucher, A. Vettraino, S. Prospero and M. Garbelotto, 2008. Reconstruction of the sudden oak death epidemic in California through microsatellite analysis of the pathogen *Phytophthora ramorum*, *Molecular Ecology*, 10.1111/j.1365–294X.2008.03773.x.

McGarigal, K., S.A. Cushman, M.C. Neel, and E. Ene, 2002. *Fragstats: Spatial Pattern Analysis Program for Categorical Maps*.

McPherson, B.A., S.R. Mori, D.L. Wood, A.J. Storer, P. Svihra, N.M. Kelly, and R.B. Staniford, 2005. Sudden oak death in California: Disease progression in oaks and tanoaks, *Journal of Forest Ecology and Management*, 213(1–3):71–89.

Pinder, J.E., and K.W. McLeod, 1999. Indications of relative drought stress in longleaf pine from Thematic Mapper data, *Photogrammetric Engineering & Remote Sensing*, 65(4):495–501.

Pu, R., M. Kelly, G.L. Anderson, and P. Gong, 2008. Using CASI hyperspectral imagery to detect mortality and vegetation stress associated with a new hardwood forest disease, *Photogrammetric Engineering & Remote Sensing* 74(1):65–75.

R Development Core Team, 2008. *R: A Language and Environment of Statistical Computin*g, Refractions Research, 2005, PostGIS.

Rizzo, D., M. Garbelotto, J.M. Davidson, G.W. Slaughter, and S.T. Koike, 2002. *Phytophthora ramorum* as the cause of extensive mortality of *Quercus* spp. and *Lithocarpus densiflorus* in California, *Plant Disease*, 86(3):205–213.

Rizzo, D.M., and M. Garbelotto, 2003. Sudden oak death: Endangering California and Oregon forest ecosystems, *Frontiers in Ecology and the Environment*, 1(5):197–204.

SAS Institute, Inc., 2005. *JMP 5.1.2*.

Shoemaker, D.A., C.B. Oneal, D.M. Rizzo, and R.K. Meentemeyer, 2008. Quantification of sudden oak death tree mortality in the Big Sur ecoregion of California, *Proceedings of the Sudden Oak Death Third Science Symposium*, 05–09 March 2007, Santa Rosa, California (U.S. Department of Agriculture, Albany, California).

Sun, W., M. Kelly, and P. Gong, 2005. Separation of dead tree crowns from oak woodland forest mosaic by integrating spatial information, *GeoCarto International*, 20(2):15–20.

Swiecki, T.J., and E. Bernhardt, 2001. Evaluation of stem water potential and other tree and stand variables as risk factors for *Phytophthora ramorum* canker development in coast live oak, *Proceedings of the Fifth California Oak Symposium*, 22–25 October, San Diego, California (U.S. Department of Agriculture, Albany, California), pp. 787–798.

van Aardt, J.A.N., and R.H. Wynne, 2004. A multi-resolution approach to forest segmentation as a precursor to estimation of volume and biomass by species, *Proceedings of the American Society for Photogrammetric Engineering and Remote Sensing Annual Conference*, 24–28 May, Denver, Colorado, (American Society for Photogrammetry & Remote Sensing, Bethesda, Maryland), unpaginated CD-ROM.

Worboys, M.F., 1992. A model for spatio-temporal information, *Proceedings of the 5th International Symposium on Spatial Data Handling*, Charleston, South Carolina, pp. 602–611.

Yamamoto, S.-I., 1993. Gap characteristics and gap regeneration in a subalpine coniferous forest on Mt. Ontake, central Honshu, Japan, *Ecological Research*, 8:277–285.

Yu, Q., P. Gong, N. Clinton, M. Kelly, and D. Schirokauer, 2006. Object-based detailed vegetation classification with airborne high resolution remote sensing imagery, *Photogrammetric Engineering & Remote Sensing*, 72(7):799–811.

Yuan, M. 1999. Use of a three-domain representation to enhance GIS support for complex spatiotemporal queries, *Transactions in GIS*, 3(2):137–159.